Post-PET ultrasound improves specificity of 18F-FDG-PET for recurrent differentiated thyroid cancer while maintaining sensitivity

Martin Biermann[1,2], Jostein Kråkenes[2,3], Katrin Brauckhoff[4], Hans Kristian Haugland[5], Achim Heinecke[6], Lars A Akslen[2,7], Jan Erik Varhaug[4,8] and Michael Brauckhoff[4,8,*]

Abstract

Background: Positron emission tomography (PET) using fluor-18-deoxyglucose (18F-FDG) with or without computed tomography (CT) is generally accepted as the most sensitive imaging modality for diagnosing recurrent differentiated thyroid cancer (DTC) in patients with negative whole body scintigraphy with iodine-131 (I-131).

Purpose: To assess the potential incremental value of ultrasound (US) over 18F-FDG-PET-CT.

Material and Methods: Fifty-one consecutive patients with suspected recurrent DTC were prospectively evaluated using the following multimodal imaging protocol: (i) US before PET (pre-US) with or without fine needle biopsy (FNB) of suspicious lesions; (ii) single photon emission computed tomography ($\geq$3 GBq I-131) with co-registered CT (SPECT-CT); (iii) 18F-FDG-PET with co-registered contrast-enhanced CT of the neck; (iv) US in correlation with the other imaging modalities (post-US). Postoperative histology, FNB, and long-term follow-up (median, 2.8 years) were taken as composite gold standard.

Results: Fifty-eight malignant lesions were identified in 34 patients. Forty lesions were located in the neck or upper mediastinum. On receiver operating characteristics (ROC) analysis, 18F-FDG-PET had a limited lesion-based specificity of 59% at a set sensitivity of 90%. Pre-US had poor sensitivity and specificity of 52% and 53%, respectively, increasing to 85% and 94% on post-US, with knowledge of the PET/CT findings ($P < 0.05$ vs. PET and pre-US). Multimodal imaging changed therapy in 15 out of 51 patients (30%).

Conclusion: In patients with suspected recurrent DTC, supplemental targeted US in addition to 18F-FDG-PET-CT increases specificity while maintainin sensitivity, as non-malignant FDG uptake in cervical lesions can be confirmed.

[6]Institute of Biostatistics and Clinical Research, University of Münster, Münster/Germany
[7]Centre for Cancer Biomarkers CCBIO, University of Bergen, Bergen/Norway
[8]Department of Clinical Science, University of Bergen, Bergen/Norway

*Professor Michael Brauckhoff died suddenly on 10 September 2014, shortly before the completion of this manuscript.

Corresponding author:
Martin Biermann, Nuclear Medicine/PET Center, Department of Radiology, Haukeland University Hospital, Jonas Liesvei, N-5021 Bergen, Norway.
Email: martin.biermann@k1.uib.no

[1]Nuclear Medicine/PET Center, Department of Radiology, Haukeland University Hospital, Bergen/Norway
[2]Department of Clinical Medicine, University of Bergen, Bergen/Norway
[3]Section for Neuroradiology, Department of Radiology, Haukeland University Hospital, Bergen/Norway
[4]Section for Endocrine Surgery, Haukeland University Hospital, Bergen/Norway
[5]Department of Pathology, Haukeland University Hospital, Bergen/Norway

Introduction

Differentiated thyroid cancer (DTC), the most common malignant endocrine tumor, generally has a favorable prognosis (1). Some patients, however, experience adverse outcomes despite improvements in preoperative imaging and surgical techniques (2,3).

In most patients with recurrent disease after previous total thyroidectomy with or without subsequent ablative radioiodine therapy (RIT), serum human thyroglobulin (hTg) will be detectable as a tumor marker. Conventional imaging including cervical ultrasound (US) and computed tomography (CT) is negative in many cases. Additional tumor lesions may be detected by iodine-131 (I-131) scintigraphy, particularly after application of a therapeutic activity of I-131 (4). In selected patients, I-131 therapy may be curative (5). In many patients, however, tumor lesions cease to take up relevant amounts of iodine. In a seminal paper in 1996, Feine showed that positron emission tomography (PET) with fluor-18-deoxy-glucose (FDG) demonstrated thyroid cancer lesions undetectable by I-131-scintigraphy (6). Highly differentiated thyroid cancer cells exhibit iodine uptake due to the expression of sodium-iodide symporter (NIS) but most often no significant glucose uptake, while less differentiated cells that ceased to express NIS upregulate glucose and FDG uptake (7–9). 18F-FDG-PET has therefore become a mainstay in the diagnosis of recurrent thyroid cancer, in particular in patients with elevated serum hTg and negative I-131 scintigraphy (10–14).

While US is the undisputed first choice in the routine evaluation and follow-up of thyroid cancer patients (10–12,15,16), its role relative to 18F-FDG-PET is less well established. We set out to determine the incremental diagnostic value of targeted cervical US performed after hybrid radionuclide imaging (FDG-PET-CT and I-131 single photon emission computed tomography + CT = SPECT-CT) (17) in a prospective cohort of 50 consecutive patients against composite gold standard based on histology, cytology, imaging, and clinical follow-up.

Material and Methods

Patient cohort. Between June 2009 and January 2012, 51 consecutive patients with suspected recurrent or progressive DTC after previous ablative therapy including total thyroidectomy (TT) and radioiodine ablation were prospectively included. Indications for multimodal imaging were (one indication per patient): suspicious US lesion(s) in 16 patients (31%) (including five already confirmed by US-guided fine needle biopsy [FNB] 10%); increasing/unexplained hTg in 20 patients (39%); restaging of known metastatic disease in five patients (10%); positive TgAB in two patients (4%); and other indications in eight patients (16%).

Imaging protocol. The multimodal imaging protocol comprising US, I-131-SPECT-CT, 18F-FDG-PET, and US-guided FNB is outlined in Table 1. US was performed by a single experienced operator (MBi) with 10 and 13 MHz linear probes on a Hitachi EUB 5500, and – from February 2011 – a Hitachi Preirus (Hitachi Medical Corp., Akihabara, Japan). FNB was performed by the same operator using a modification of Zajdela's capillary sampling technique (18). Under US guidance, 0.4×88 mm spinal needles (Braun Spinocan; B. Braun AG, Melsungen, Germany) were advanced to the border of the lesion. The stylus was then withdrawn by an assistant and the needle moved inside the lesion. Sampled material was smeared on glass slides. Airdried specimens were stained with Giemsa and ethanol fixed specimens with Papanicolaou stain. Three or four FNBs were performed for each lesion. From February 2011, washout from the biopsy needles rinsed with 0.5 mL 0.9% sodium chloride solution was additionally analyzed for hTg and TgAB using the same assays as for serum samples (19). Post-PET US was performed for supplementary biopsy or when multimodal imaging showed extra lesions that had not been diagnosed on the pre-PET US examination.

I-131-SPECT-CT was performed on a Siemens Symbia T6 (Siemens Healthcare, Erlangen, Germany) with high-energy collimators. After a whole body planar scan, SPECT of the neck and upper mediastinum was taken (2×32 projections @ 20 s) with a co-registered low-dose CT (130 kV, effective tube current 15 mAs).

18F-FDG-PET was performed on a Siemens Biograph 40 (Siemens Healthcare) after an overnight fast. Approximately 60 min after injection of approximately 370 MBq 18F-FDG, a whole-body PET was acquired from the skull to the thighs at 3 min per bed position after an initial low-dose CT (120 kV, 50 mAs)

Table 1. Imaging protocol.

Day	Procedure(s)
1	Ultrasound, TSH, hTg, hTg-AB rhTSH i.m.
2	rhTSH i.m.
3	Oral I-131 ($\geq$3 GBq)
6	I-131 SPECT-CT
7	18F-FDG-PET with dedicated CECT/PET of the neck US (if new findings on PET-CT), FNB of 1 index lesion

CECT, contrast-enhanced CT (alternatively diagnostic CT without intravenous contrast in patients with therapeutically relevant I-131 uptake).

(20). A dedicated PET-CT of the neck and upper mediastinum was then performed with the arms down at 6 min per bed with a co-registered contrast-enhanced CT (CECT; 120 mV, 240 mAs; 2 mm slices, field of view 240 mm) acquired 50 s after intravenous injection of 100 mL iomeprol (350 mg iodine/mL; Bracco Imaging Scandinavia, AB, Gothenburg, Sweden).

For stimulation with thyroid stimulating hormone (TSH), patients either received intramuscular injections of 0.9 mg recombinant human TSH (rhTSH, Thyrogen®; Genzyme Corp., Cambridge, MA, USA) on two successive days, or thyroid hormone was withdrawn for 4 weeks.

Image processing and analysis. All image data including US were digitally archived in the department's Picture Archiving and Communication System (PACS) (Agfa Impax 6, Agfa Healthcare BV, Antwerp, Belgium). US lesions were classified according to current consensus criteria (21). CTs were read on PACS workstations using calibrated screens. Nuclear medicine data were processed with Segami Oasis (v. 1.9.3; Segami Corporation, Columbia, MD, USA). Maximum SUV (SUV_{max}) in PET images was determined by placing spherical volumes of interest (VOI) around each focus, preferentially in the dedicated cervical acquisition. In case of neighboring hot lesions, custom VOIs were drawn. Lesions were classified as FDG-positive when the SUV was ≥ 2.5 or when a focus was clearly discernible against the background (22,23). I-131 uptake was assessed using a 5-point qualitative scale (less than background, background, faint, warm, hot).

Clinical chemistry. Serum thyroglobulin (hTg) and anti-thyroglobulin antibodies (TgAB) were analyzed by immunometric assays (Immulite 2000) from Siemens Healthcare Diagnostics (Llanberis, UK), urinary iodide based on the Sandell-Kolthoff reaction.

Surgery. Compartment-oriented microdissection with systematic removal of lymphatic and fatty tissue was performed under general anesthesia (24,25). When the compartment had already been extensively dissected, recurrent tumor was resected without systematic compartment dissection. Neural monitoring was undertaken for all relevant nerves including the recurrent laryngeal, vagus, accessory, phrenic, and hypoglossal nerves (26,27).

Histopathology. Tissues were fixed in 10% neutral buffered formalin for 2–3 days. Lymph nodes were bisected along the hilar plane. Five μm sections of samples embedded in paraffin were stained by Hematoxylin and Eosin (HE), supplemented by immunohistochemical staining for thyroglobulin in selected cases.

Follow-up. All patients were followed with the imaging modalities that had been positive on the original multimodal imaging protocol. A composite gold standard was based on the best available evidence (histology, cytology, repeat imaging, and/or clinical follow-up in descending order). Individual findings ("lesions") were classified as true/false positive/negative as reported at the time of the original study in relation to the composite gold standard (22). On the patient level, multimodal imaging was scored as true positive (TP) if at least one TP lesion was detected, as false positive (FP)/false negative (FN) in case of at least one FP/FN lesion in the absence of TP lesions, and otherwise as true negative (TN). All original image studies were re-read to detect FN findings overlooked at the time of the original report.

Ethics. The project was conducted as a quality surveillance study in full accordance with the guidelines issued by the institutional review board (IRB) and current Norwegian legislation, and the IRB exempted the study from review on 28 February 2014.

Data management, analysis, and statistics. All observations were registered in MDcake, a client-server database application developed by our group for the present study (28,29). Multiple lesions in parenchymatous organs such as lung or liver were encoded as a single lesions to avoid biasing lesion-based analysis. Data were re-aggregated into two SQL views, one for analyzing patients/studies and one for lesions. These provide the basis for all subsequent analyses. These were conducted with the statistics program "R" (30). For group comparisons, Wilcoxon rank sum test and Fisher's exact test were applied at a significance level of 5% (two-sided).

To evaluate the performance of diagnostic modalities with a continuous (FDG SUV) or ordinal predictor (I-131 uptake), receiver operating characteristics (ROC) analysis was performed with R package pROC. The likelihood of a correct diagnosis of a tumor lesion (sensitivity) is plotted against the likelihood of an incorrectly diagnosed benign lesion (1 – specificity) for all possible values of the predictor. For an ideal method, the ROC curve will approach the upper left corner of the plot while the curve will be close to the diagonal for a method with low predictive power. Ninety-five-percent confidence intervals (CI) for sensitivity and area under the curve (AUC) were calculated by bootstrapping (2000 iterations) (31).

Table 2. Patients summary.

Parameter	All patients, $n = 51$ (%)	Disease, $n = 33$ (65%)	Disease-free, $n = 18$ (35%)	
Female	29 (57%)	18 (53 %)	11 (65 %)	
Age (years)*	56 (44–69)	62 (55–75)	52 (38–54)	$P < 0.002$
Age at diagnosis (years)	51 (35–60)	53 (42–65)	36 (30–50)	$P < 0.002$
Haukeland UH	35 (69%)	22 (65%)	13 (77%)	
Papillary TC	41 (80%)	25 (76%)	16 (89%)	
TNM group > II	32 (67%)	25 (74%)	7 (41%)	$P < 0.02$
Completed TT	51 (100%)	33 (100%)	18 (100%)	
Sum I-131 (GBq)	5.6 (3.0–5.6) [0–30]	5.6 (3.0–5.8) [0–28]	4.0 (2.2–5.6) [0.2–30]	
Re-operation	13 (26%)	8 (24%)	5 (28%)	
Time since TT (years)	4.2 (2.0–10) [0.4–30]	4.0 (2.3–9.5) [0.4–22]	6.4 (1.3–11) [0.5–30]	
hTg (suppressed) (µg/L)	0.9 (0–12) [0–903]	6.7 (0.9–37) [0–903]	0.0 (0.0–0.4) [0.0–0.9]	$P < 0.001$
hTg (stimulated) (µg/L)	8.8 (1.3–40) [0–7386]	22 (5–85) [0–7386]	1.6 (0.1–4.6) [0–19]	$P < 0.001$
hTg AB	4 (8%)	2 (6%)	2 (12%)	
rTSH	45 (88%)	29 (88%)	16 (89%)	
Urinary iodide (µg/L)	113 (80–128) [29–159]	117 (80–128) [29–159]	103 (85–113) [74–134]	
Follow-up (years)	2.8 (1.7–3.4) [0.1–4.9]	2.9 (1.7–3.4) [0.1–4.9]	2.5 (2.1–3.5) [1.2–4.5]	

Patient characteristics according to disease state. Distributions are tabulated as median (interquartile range) [range].
*Age at the time of multimodal imaging (MMI).
Haukeland UH, primary surgery at Haukeland University Hospital; hTg, human thyroglobulin; I-131, cumulative activity of I-131 before MMI; papillary TC, papillary thyroid cancer; Re-operation, re-operated before MMI; TNM group, TNM stage grouping; TT, thyroidectomy.

Results

Patient-based analysis. Multimodal imaging was TP in 32 patients, TN in 16, FP in 2, and FN in 1, yielding a sensitivity of 97% (95% CI, 94–99) and specificity of 89% (95% CI, 65–99). Patient characteristics are summarized in Table 2 and shown in detail in Supplementary Table 1 (published online only).

Lesion-based analysis. Eighty-six conspicuous lesions were found in 43 patients (Table 3; see also Supplementary Table 2, published online only). Fifty-eight lesions were TP, 19 TN, five FP, and four FN, yielding a diagnostic accuracy of 90%, a sensitivity of 94% (95% CI, 84–98), and a specificity of 79% (95% CI, 58–93).

Fifty-seven lesions located in the neck or upper mediastinum accessible to US (in short: "neck lesions") were analyzed in detail. On ROC analysis, I-131-imaging lacked predictive power with an AUC of 0.51 (95% CI 0.44 – 0.58) for neck lesions and 0.55 (0.46–0.64) for all lesions (Fig. 1). FDG-PET had high discriminative power with an AUC of 0.80 (0.67 – 0.93) for neck lesions and 0.68 (0.56 – 0.80) for all lesions. However, at high sensitivities FDG-PET showed poor specificity. The inclusion of CECT in the workup achieved a high sensitivity of 90 % (76–97) with improved specificity of 71 % (44 – 90) compared with 58 % (9 – 88) of FDG-PET alone at the same level of sensitivity, but without reaching statistical significance. US before PET including optional FNB (preUS) had limited accuracy of 53 % with a sensitivity of 53 % (36 – 69 %) and a specificity of 53 % (28 – 77 %) (Figs 2 and 3 for examples). US in the detailed knowledge of the findings on PET-CT and SPECT-CT (postUS) out-performed PET alone and preUS with a specificity of 94 % (71 – 99) while maintaining sensitivity at 85 % (70 – 94) (p < 0.05 for all comparisons).

To estimate the relative contribution of US with and without FNB to overall diagnostic performance, we simulated an imaging workflow as outlined in Table 1 with FNB being performed only as the last step of the protocol. Of the 40 malignant neck lesions, pre-US without FNB would have correctly diagnosed 18 lesions (45%), and pre-US plus radionuclide imaging another 18 (45%). Post-US and FNB did not increase the diagnostic yield over the combination of pre-US and PET-CT, while four malignant lesions remained undetected. Of the 17 benign neck lesions, nine (50%)

Table 3. Lesions summary.

Region	Malignancy	Lesion type*	n	FDG-pos.	I-131-pos.	Volume (mL)	SUV$_{max}$	Patients[†] (n)	
Neck (n = 57)	Malignant	Local recurrence	6	6 (100%)	0	0.4 (0.2–0.7)	7.0 (3-12) [0–49][‡]	5	22
		LN	34	27 (82%)	4 (12%)			21	
	Benign	LN	17	6 (35%)	0	0.4 (0.2–0.9)	1.9 (0-4) [0–11][‡]	12	12
Body (n = 29)	Malignant	Mediastinum LN	3	2	1	1.3 (0.2–3.5)	2.8 (1-6) [0–20]	3	15
		Lung metastases	9	4	2			9	
		Bone metastases	9	2	8			3	
		Other metastases	1	1	0			1	
	Benign	Thymus	4	4	3	3.4 (0.9–7.3)	5.0 (3-6) [1–7]	2	5
		Other	3	1	0			3	

Lesion characteristics according to anatomical region: type of lesion, number of lesions (n), FDG uptake, I-131 uptake, lesion volume in mL (median, interquartile range), SUV$_{max}$ (median, interquartile range, [range]).
*Lymph node metastases (LN) in neck and upper mediastinum accessible to cervical US (Neck) and mediastinum, distant metastases.
†Number of patients affected.
‡$P < 0.001$ (Wilcoxon rank test).
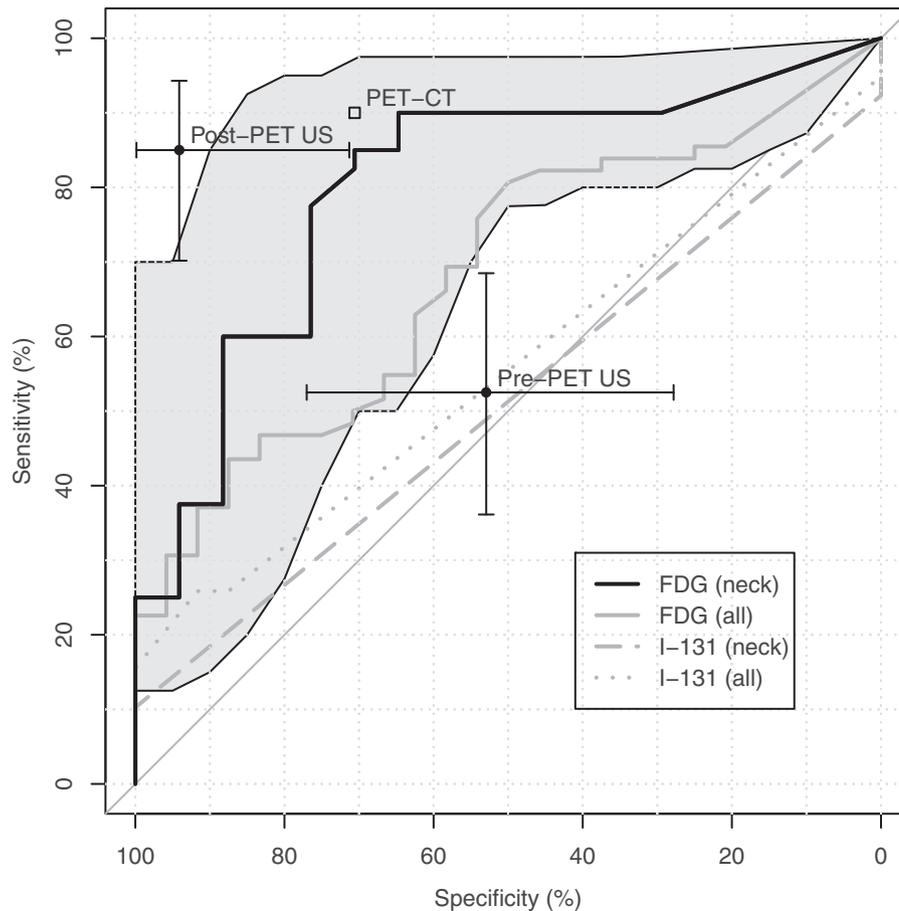
Fig. 1. ROC analysis. For 18F-FDG-PET (FDG) and I-131 scintigraphy (I-131) in neck lesions (neck) or the entire body (all) sensitivity is plotted against specificity for all possible values of the predictor (standardized uptake value or intensity of I-131 uptake). The performance of US before PET (Pre-PET) and after PET (Post-PET) as well as the performance of PET-CT are plotted as discrete data points. Error bars and the gray area around the curve for FDG-PET in the neck indicate 95% confidence intervals.
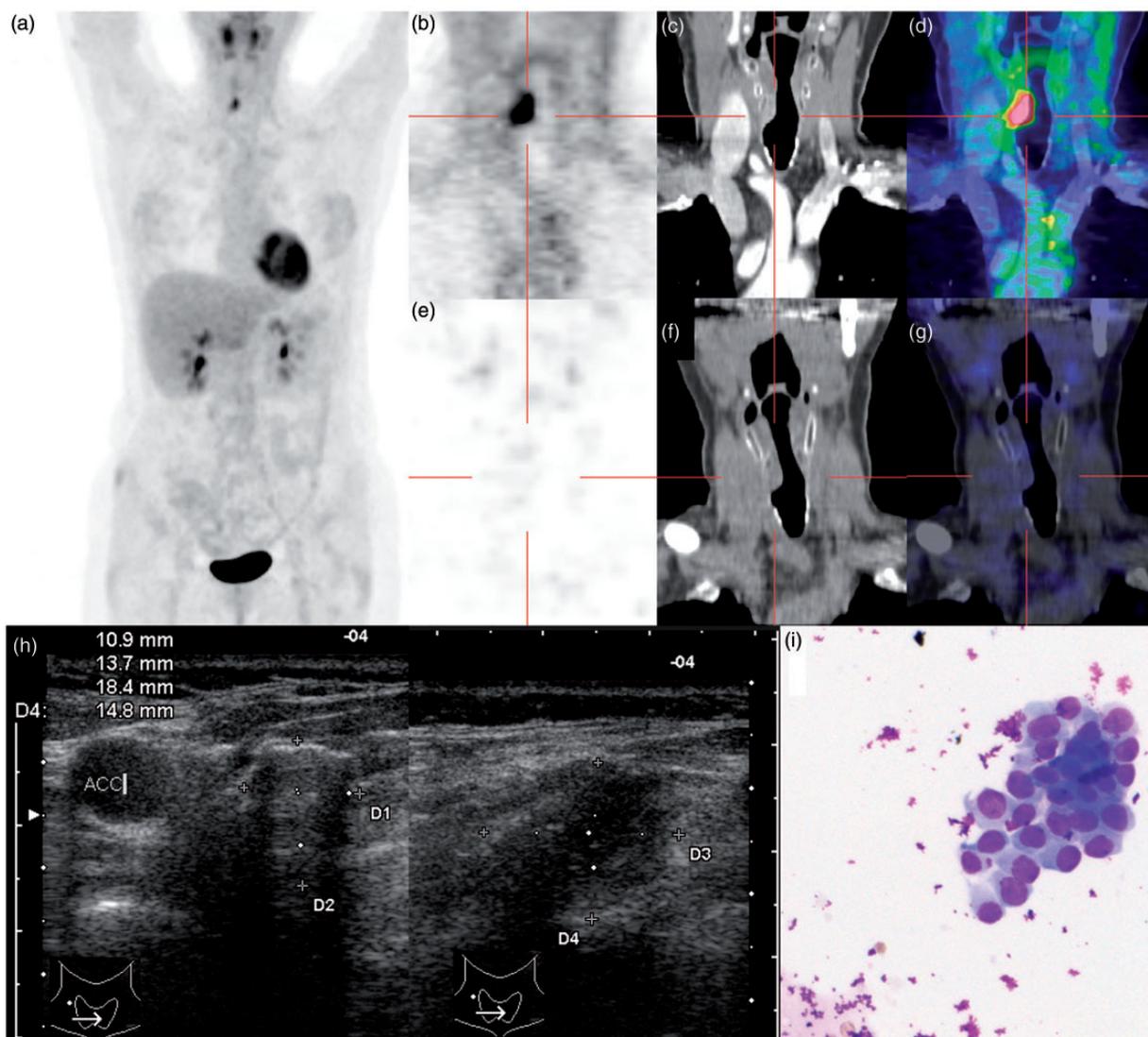
Fig. 2. A 59-year-old patient with unclear rise of hTg. Previous imaging including repeated ultrasound of the neck was negative. 18F-FDG-PET-CT revealed a paralaryngeal recurrence: Whole-body PET (a), coronal PET slice (b), contrast-enhanced CT (c), and fusion image (d). I-131-SPECT-CT showed no corresponding uptake (e–g). US after PET revealed an hypoechoic soft tissue lesion (h). US-guided FNB showed abnormal epithelial cells (i). The patient was treated by endotracheal laser ablation.

were TN on pre-US and PET-CT while eight (44%) were FDG-positive. Three (17%) required post-US and another three (17%) FNB to establish the correct diagnosis (sparing three patients for unnecessary compartment resections for benign disease) while two remained FP, one of them with a FP FNB.

Outcomes. Multimodal imaging correctly changed the original therapy assignment in 15 out of 51 patients (30%) (Table 4). Twenty-four patients underwent surgery, eight in the central compartment, 11 in at least one lateral compartment, four in the upper mediastinum (three necessitating sternotomy), and four for distant metastases (two lung, one adrenal, one hip). Patients were followed for a median 2.5 years. Two patients

died unrelated to thyroid cancer. Seven patients had progressive disease, seven patients had stable disease, all in the group with TP imaging. No recurrences occurred in the 15 MMI negative patients with exception of patient 20 (Fig. 4). All other patients are in complete remission.

Discussion

High-resolution US is the mainstay of the assessment of thyroid cancer both for initial evaluation and for follow-up (10–12,15,16). US may help avoid repeat surgery in up to 40% of patients when compared with physical examination alone (32,33).

The incremental value of US over other imaging modalities is more difficult to ascertain. To our
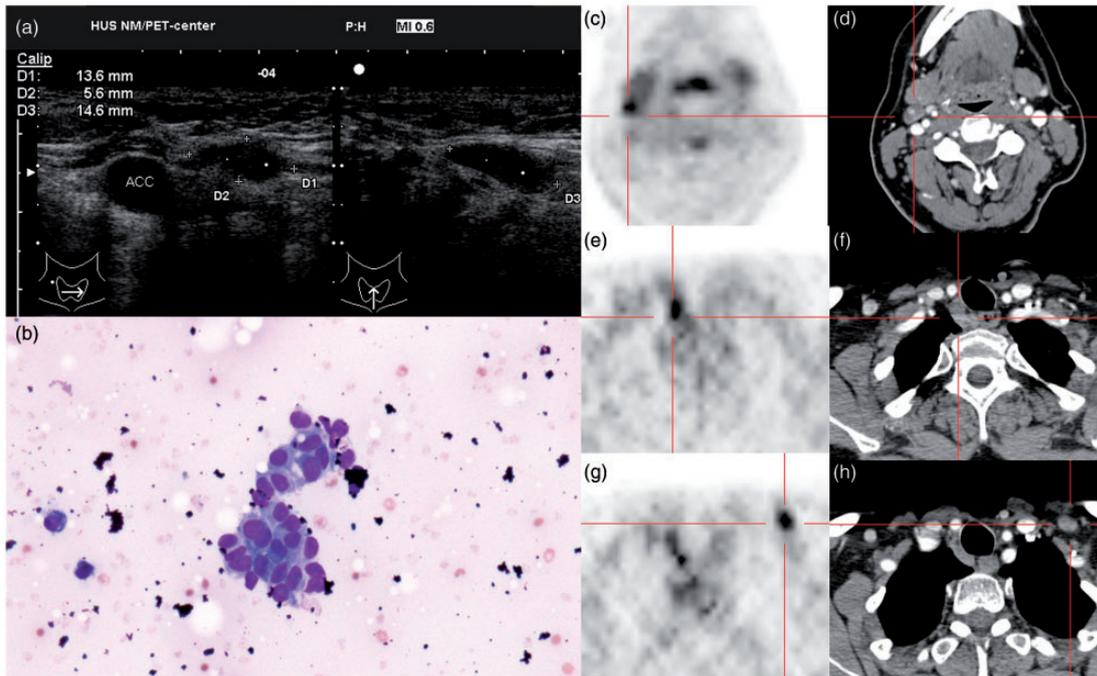
Fig. 3. A 54-year-old patient with cytologically confirmed index lesion. Routine US September 2009 revealed a hypoechoic lymph node behind the left clavicle (a). Cytology showed abnormal epithelium – papillary thyroid cancer (b). As expected, PET-CT showed FDG uptake (SUV_{max} 6.4) in the index lesion (panels g, h). In addition it revealed a right-sided paratracheal recurrence (SUV_{max} 7.0) that was not visible on US (e, f) and a cystic lymph node metastasis behind the right angle of the jaw (SUV 5.0) that had been overlooked on initial US. The patient was re-operated with a revision of the cranial right lateral neck (K2/II), the right-sided central compartment (K1b/IV), and the caudal left lateral neck (K3/V) with preservation of recurrent laryngeal nerve function. All lesions were histologically confirmed.

Table 4. Therapeutic consequence of multimodal imaging.

Therapy pre	Therapy post multimodal imaging incl. post-US					Σ
	Follow-up*	I-131[†]	Surgery[‡]	Extended surgery[§]	Palliative treatment**	
Follow-up*	20	1	3	4	2	30
I-131[†]		3				3
Surgery[‡]	1		7	3		11
Extended surgery[§]	1			3		4
Palliative treatment**						0
Σ	22	4	10	10	2	48

*Continuation of follow-up.
†Radioiodine therapy.
‡Surgery in a single cervical compartment.
§Extended surgery (at least one more cervical compartment than originally planned).
**Palliative treatment = external beam radiotherapy and endotracheal laser ablation in one patient each.
The line of identity is emphasized in gray. The 13 patients in the white area to the upper right received more aggressive therapy than planned. Two patients in the white area to the lower left were downstaged and assigned to follow-up without surgery. The two patients with FP imaging (Follow-up→Surgery) and the one patient with FN imaging (Follow-up→Follow-up) are not listed.

knowledge, our series is the first to systematically evaluate the performance of US before and after multimodal sectional imaging – I-131 SPECT-CT and 18F-FDG PET-CT – by the same observer in the same cohort of patients with known or suspected recurrent DTC. In our prospective analysis of 51 consecutive patients, US with optional FNB before radionuclide imaging identified only 53% of all cancer lesions in the neck, while US after multimodal imaging had a significantly higher lesion based sensitivity of 85% ($P < 0.05$). US after multimodal imaging had the highest specificity of 94% versus 53% for US alone and 80% for
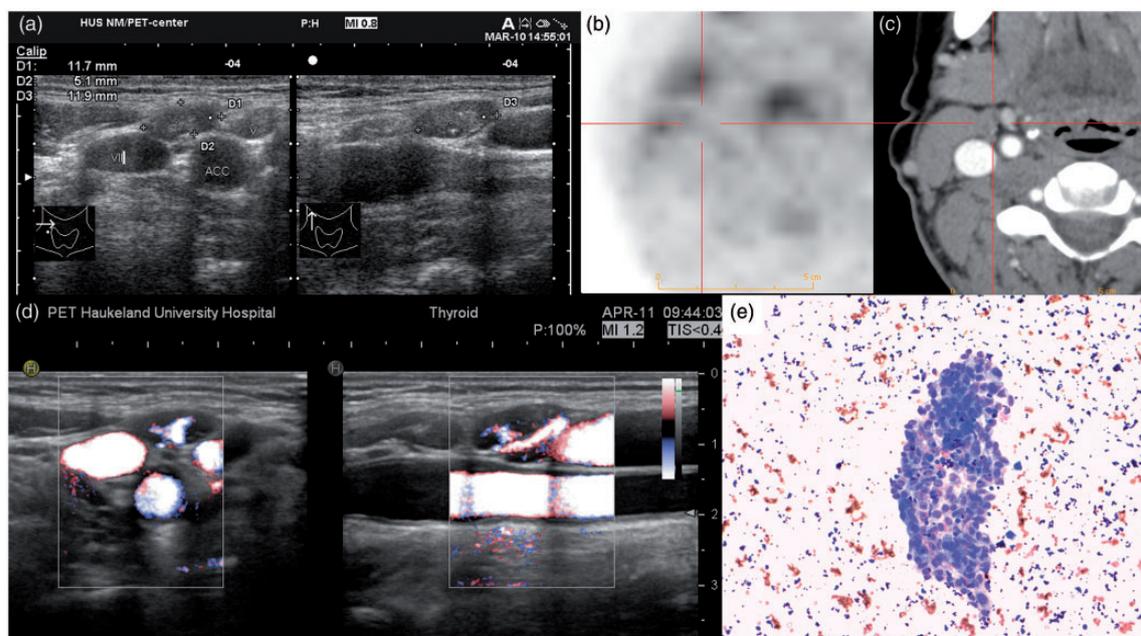
Fig. 4. FN multimodal imaging in a 49-year-old patient. Routine US had detected a suspicious lymph node behind the right angle of the jaw with microcalcifications (a). 18F-FDG-PET (b, c) and I-131-SPECT-CT (not shown) showed no tracer uptake. US-guided FNB was FN. On repeat imaging with new US machine (d), the lymph node showed focal hyperperfusion not observed in the surrounding nodes. New cytology was positive (e) with a human thyroglobulin in the washout from the needle of 855 ng/L. FDG-PET was still negative (not shown). Re-operation revealed one metastasis in 21 lymph nodes.

18F-FDG-PET alone ($P < 0.05$). High specificity is necessary to avoid futile surgery based on FP findings. In a simulated workflow assuming FNB as the last step in the diagnostic algorithm, pre-US and radionuclide imaging together would have identified 90% of all malignant neck lesions with no further increase in sensitivity by post-US and FNB. Post-US and FNB were, however, vital for the correct diagnosis of benign lesions with non-malignant reactive or inflammatory FDG uptake, increasing specificity from 50% for PET-CT alone to 90% for PET-CT + post-US + FNB. We therefore strongly recommend post-US with optional FNB for the evaluation of all FDG-positive neck lesions in patients with thyroid cancer, at least when surgery is considered. For the evaluation of clinically suspicious neck lesions and for routine follow-up, US supplanted by FNB up front is the most efficient first-line imaging modality: FNB of an index lesion will quickly establish or refute the indication for further imaging or therapeutic intervention, while it will also establish the correct diagnosis of malignancy in lesions that would be missed by PET-CT alone.

The main imaging modality chosen for the evaluation of US was 18F-FDG-PET as it is the most sensitive imaging method for the evaluation of recurrent DTC. In a systematic meta-analysis performed by Dong et al. in 2009, FDG-PET had a pooled lesion-based sensitivity of 91.6% and a patient-based sensitivity of 88.5% in patients with elevated hTg and negative I-131 scintigraphy (14). Specificity of FDG-PET was, however, limited to 77.5% (lesion-based) and 84.7% (patient-based), which compares well with our own results.

We were disappointed by the performance of cervical US when performed alone (pre-US). The most detailed head-to-head comparison of US and FDG-PET was performed by Seo et al. (34). In 20 thyroid cancer patients (19 PTC, 1 MTC) with cytologically proven recurrence, US, CECT, and PET-CT were compared with histology in each of 110 nodal levels that were surgically explored. Sensitivity and specificity for US was 69.2% and 89.7% for CECT 63.5% and 94.8%, and for PET-CT 53.8% and 79.3%. These findings based on histology as the sole gold standard are largely in agreement with ours. The sensitivity of US is likely overestimated, since only patients with positive FNB of at least one cervical lesion were included.

Only a few studies allow estimates of the sensitivity of US when performed independently of 18F-FDG-PET. In a series with 49 patients with DTC and positive serum hTg, only one out of six local recurrences was found on pre-PET US while five were seen on CECT and PET. All were confirmed by hTg in US-guided FNB after PET (35). In a recent multicenter series

with 327 patients, per-patient sensitivity and specificity was 37% and 94% for US, and 92% and 95% for PET/CT (36). In a single-center study in 423 patients, 16 out of 90 recurrent lesions were missed on US, but diagnosed with FDG-PET-CT (23).

Our observation that cervical US misses cancerous lesions is further confirmed by studies that only included patients with negative conventional imaging including US. In a series of 34 patients with 30 tumor lesions in the neck, new US detected 18 (including three that were FDG-negative), CECT 14, and FDG-PET 27 (37). In another recent prospective series, FDG-PET/CT had a per-patient sensitivity of 87%, and a specificity of only 77% implying that the majority of the lesions had been overlooked at baseline US (38). Similar observations were made by Pomerri et al. (39) and Freudenberg et al. (40).

There are limitations connected to our study. Ideally, the standard for evaluating a diagnostic method should be completely independent of the method under study (41). A correct estimate of the specificity of a diagnostic method and its positive predictive value requires also a sufficient number of negative observations (42). If histological specimens were taken as sole gold standard, the last condition can only be met if prophylactic lymph node dissection is performed even in the absence of disease demonstrable by imaging. In a series of 560 patients by Ito, US had a per patient sensitivity of 27.2% and a specificity of 96.5% compared with histological specimens (43). Preliminary results from our own series and a smaller recent study (44) confirm that imaging underestimates the number of malignant lesions compared with histological preparations. Results from Ito's series (43,45) imply that micrometastases in cervical lymph nodes do not have the same prognostic relevance as macrometastases that are detected clinically or by cervical US. Thus measuring the performance of cervical US against histology may not lead to appropriate conclusions for the clinical management of patients with DTC.

Misdiagnoses in two patients in our series could have probably been avoided, if we had analyzed hTg from the washout of the US-guided FNB as we did from February 2011. The thymic lesions were unfortunately inaccessible to percutaneous biopsy.

The proportion of patients with iodine-avid lesions in our cohort was lower than in a recent German series, in which 78 out of 327 patients (24 %) had TP findings on I-131 scintigraphy (37). In two recent series from France and Italy, only one out of 34 hTg-positive patients had therapeutically relevant I-131 uptake (37), and only one of 22 patients had therapeutically relevant uptake in a pulmonary metastasis (46). Measurements of urinary iodine excretion in our patients exclude iodine contamination as a cause for

our observation. As a consequence of this study, we have altered our protocol from combined imaging/therapy with ≥ 3 GBq I-131 to imaging with I-123, a pure gamma emitter, in order to reduce radiation exposure particularly to the salivary glands (47).

In conclusion, in patients evaluated for recurrent DTC after previous ablative therapy US performed independent of other imaging modalities misses about half of cancer lesions in the neck while 18F-FDG-PET is sensitive but lacks specificity. US performed in correlation with 18F-FDG-PET-CT maintained the sensitivity of FDG-PET, but increased specificity by eliminating false positive diagnoses due non-malignant FDG uptake in cervical lesions.

Supplementary material

Supplementary material is available online at acr.sagepub.com/supplemental.

References

1. Cancer Registry of Norway. *Cancer in Norway 2012. Cancer incidence, mortality, survival and prevalence in Norway*. Oslo: Cancer Registry of Norway, 2014. Available at: http://www.kreftregisteret.no/en/
2. Brauckhoff M, Machens A, Thanh PN, et al. Impact of extent of resection for thyroid cancer invading the aerodigestive tract on surgical morbidity, local recurrence, and cancer-specific survival. Surgery 2010;148:1257–1266.
3. Biermann M, Pixberg M, Riemann B, et al. Clinical outcomes of adjuvant external-beam radiotherapy for differentiated thyroid cancer - Results after 874 patient-years of follow-up in the MSDS-trial. Nuklearmedizin 2009;48: 89–98.

4. Maxon HR. Detection of residual and recurrent thyroid cancer by radionuclide imaging. Thyroid 1999;9:443–446.

5. Durante C, Haddy N, Baudin E, et al. Long-term outcome of 444 patients with distant metastases from papillary and follicular thyroid carcinoma: benefits and limits of radioiodine therapy. J Clin Endocrinol Metab 2006;91:2892–2899.

6. Feine U, Lietzenmayer R, Hanke JP, et al. Fluorine-18-FDG and iodine-131-iodide uptake in thyroid cancer. J Nucl Med 1996;37:1468–1472.

7. Moon SH, Oh YL, Choi JY, et al. Comparison of 18F-fluorodeoxyglucose uptake with the expressions of glucose transporter type 1 and Na+/I- symporter in patients with untreated papillary thyroid carcinoma. Endocr Res 2013;38:77–84.

8. Grabellus F, Nagarajah J, Bockisch A, et al. Glucose transporter 1 expression, tumor proliferation, and iodine/glucose uptake in thyroid cancer with emphasis on poorly differentiated thyroid carcinoma. Clin Nucl Med 2012;37:121–127.

9. Schönberger J, Rüschoff J, Grimm D, et al. Glucose transporter 1 gene expression is related to thyroid neoplasms with an unfavorable prognosis: an immunohistochemical study. Thyroid 2002;12:747–754.

10. Leenhardt L, Erdogan MF, Hegedus L, et al. 2013 European thyroid association guidelines for cervical ultrasound scan and ultrasound-guided techniques in the postoperative management of patients with thyroid cancer. Eur Thyroid J 2013;2:147–159.

11. Cooper DS, Doherty GM, Haugen BR, et al. Revised American Thyroid Association management guidelines for patients with thyroid nodules and differentiated thyroid cancer. Thyroid 2009;19:1167–1214.

12. Pacini F, Schlumberger M, Dralle H, et al. European consensus for the management of patients with differentiated thyroid carcinoma of the follicular epithelium. Eur J Endocrinol 2006;154:787–803.

13. Biermann M, Schober O. Should high hTg levels in the absence of iodine uptake be treated? Eur J Nucl Med Mol Imaging 2003;30:160–163.

14. Dong M-J, Liu Z-F, Zhao K, et al. Value of 18F-FDG-PET/PET-CT in differentiated thyroid carcinoma with radioiodine-negative whole-body scan: a meta-analysis. Nucl Med Commun 2009;30:639–650.

15. Su HK, Dos Reis LL, Lupo MA, et al. Striving toward standardization of reporting of ultrasound features of thyroid nodules and lymph nodes: A multidisciplinary consensus statement. Thyroid 2014;24:1–9.

16. Sipos JA. Advances in ultrasound for the diagnosis and management of thyroid cancer. Thyroid 2009;19:1363–1372.

17. Biermann M, Schwarzlmüller T, Fasmer KE, et al. Is there a role for PET-CT and SPECT-CT in pediatric oncology? Acta Radiol 2013;54:1037–1054.

18. Zajdela A, Zillhardt P, Voillemot N. Cytological diagnosis by fine needle sampling without aspiration. Cancer 1987;59:1201–1205.

19. Cunha N, Rodrigues F, Curado F, et al. Thyroglobulin detection in fine-needle aspirates of cervical lymph nodes: a technique for the diagnosis of metastatic differentiated thyroid cancer. Eur J Endocrinol 2007;157:101–107.

20. Boellaard R, O'Doherty MJ, Weber WA, et al. FDG PET and PET/CT: EANM procedure guidelines for tumour PET imaging: version 1.0. Eur J Nucl Med Mol Imaging 2010;37:181–200.

21. Frates MC, Benson CB, Charboneau JW, et al. Management of thyroid nodules detected at US: Society of Radiologists in Ultrasound consensus conference statement. Radiology 2005;237:794–800.

22. Vera P, Kuhn-Lansoy C, Edet-Sanson A, et al. Does recombinant human thyrotropin-stimulated positron emission tomography with [18F]fluoro-2-deoxy-D-glucose improve detection of recurrence of well-differentiated thyroid carcinoma in patients with low serum thyroglobulin? Thyroid 2010;20:15–23.

23. Seo JH, Lee SW, Ahn B-C, et al. Recurrence detection in differentiated thyroid cancer patients with elevated serum level of antithyroglobulin antibody: special emphasis on using (18)F-FDG PET/CT. Clin Endocrinol (Oxf) 2010;72:558–563.

24. Dralle H, Damm I, Scheumann GF, et al. Compartment-oriented microdissection of regional lymph nodes in medullary thyroid carcinoma. Surg Today 1994;24:112–121.

25. Tisell LE, Nilsson B, Mölne J, et al. Improved survival of patients with papillary thyroid cancer after surgical microdissection. World J Surg 1996;20:854–859.

26. Randolph GW, Dralle H, International Intraoperative Monitoring Study Group, et al. Electrophysiologic recurrent laryngeal nerve monitoring during thyroid and parathyroid surgery: international standards guideline statement. Laryngoscope 2011;121 (Suppl. 1):S1–S16.

27. Schneider R, Randolph GW, Sekulla C, et al. Continuous intraoperative vagus nerve stimulation for identification of imminent recurrent laryngeal nerve injury. Head Neck 2013;35:1591–1598.

28. Biermann M. A simple versatile solution for collecting multidimensional clinical data based on the CakePHP web application framework. Comput Methods Programs Biomed 2014;114:70–79.

29. Biermann M, Schober O. GCP-compliant management of the Multicentric Study Differentiated Thyroid Carcinoma (MSDS) with a relational database under Oracle 8i. Inform Biometr Epidemiol Med Biol 2002;33:441–459.

30. R Core Team. *R: A language and environment for statistical computing*. Vienna: R Foundation for Statistical Computing, 2014. Available at: http://www.R-project.org/

31. Robin X, Turck N, Hainard A, et al. pROC: an open-source package for R and S + to analyze and compare ROC curves. BMC Bioinformatics 2011;12:77.

32. Stulak JM, Grant CS, Farley DR, et al. Value of preoperative ultrasonography in the surgical management of initial and reoperative papillary thyroid cancer. Arch Surg 2006;141:489–494. (discussion 494–496).

33. Kouvaraki MA, Shapiro SE, Fornage BD, et al. Role of preoperative ultrasonography in the surgical

management of patients with thyroid cancer. Surgery 2003;134:946–954.

34. Seo YL, Yoon DY, Baek S, et al. Detection of neck recurrence in patients with differentiated thyroid cancer: comparison of ultrasound, contrast-enhanced CT and (18)F-FDG PET/CT using surgical pathology as a reference standard: (ultrasound vs. CT vs. (18)F-FDG PET/CT in recurrent thyroid cancer). Eur Radiol 2012;22:2246–2254.

35. Agate L, Bianchi F, Giorgetti A, et al. Detection of metastases from differentiated thyroid cancer by different imaging techniques (neck ultrasound, computed tomography and [18F]-FDG positron emission tomography) in patients with negative post-therapeutic (131)I whole-body scan and detectable serum thyroglobulin levels. J Endocrinol Invest 2014;37:967–972.

36. Riemann B, Uhrhan K, Dietlein M, et al. Diagnostic value and therapeutic impact of (18)F-FDG-PET/CT in differentiated thyroid cancer. Results of a German multicentre study. Nuklearmedizin 2013;52:1–6.

37. Leboulleux S, El Bez I, Borget I, et al. Postradioiodine treatment whole-body scan in the era of 18-fluorodeoxyglucose positron emission tomography for differentiated thyroid carcinoma with elevated serum thyroglobulin levels. Thyroid 2012;22:832–838.

38. Vural GU, Akkas BE, Ercakmak N, et al. Prognostic significance of FDG PET/CT on the follow-up of patients of differentiated thyroid carcinoma with negative 131I whole-body scan and elevated thyroglobulin levels: correlation with clinical and histopathologic characteristics and long-term follow-up data. Clin Nucl Med 2012; 37:953–959.

39. Pomerri F, Cervino AR, Al Bunni F, et al. Therapeutic impact of (18)F-FDG PET/CT in recurrent differentiated thyroid carcinoma. Radiol Med 2014;119:97–102.

40. Freudenberg LS, Antoch G, Frilling A, et al. Combined metabolic and morphologic imaging in thyroid carcinoma patients with elevated serum thyroglobulin and negative cervical ultrasonography: role of 124I-PET/CT and FDG-PET. Eur J Nucl Med Mol Imaging 2008;35:950–957.

41. Whiting PF, Rutjes AWS, Westwood ME, et al. QUADAS-2: a revised tool for the quality assessment of diagnostic accuracy studies. Ann Intern Med 2011; 155:529–536.

42. Mulla M, Schulte K-M. Terminology inaccuracies in the interpretation of imaging results in detection of cervical lymph node metastases in papillary thyroid cancer. Endocr Connect 2012;1:78–86.

43. Ito Y, Tomoda C, Uruno T, et al. Ultrasonographically and anatomopathologically detectable node metastases in the lateral compartment as indicators of worse relapse-free survival in patients with papillary thyroid carcinoma. World J Surg 2005;29:917–920.

44. Weber T, Ohlhauser D, Hillenbrand A, et al. Impact of FDG-PET computed tomography for surgery of recurrent or persistent differentiated thyroid carcinoma. Horm Metab Res 2012;44:904–908.

45. Ito Y, Tomoda C, Uruno T, et al. Preoperative ultrasonographic examination for lymph node metastasis: usefulness when designing lymph node dissection for papillary microcarcinoma of the thyroid. World J Surg 2004;28:498–501.

46. Rosario PW, Mourão GF, dos Santos JBN, et al. Is empirical radioactive iodine therapy still a valid approach to patients with thyroid cancer and elevated thyroglobulin? Thyroid 2014;24:533–536.

47. Gerard SK. Whole-body thyroid tumor 123I scintigraphy. J Nucl Med 2003;44:852.